Received: 17 December 2019 | Revised: 17 June 2020 | Accepted: 23 June 2020

DOI: 10.1096/fj.201903128RR

RESEARCH ARTICLE

THE FASEB JOURNAL

Alzheimer's disease in the gut—Major changes in the gut of 5xFAD model mice with ApoA1 as potential key player

Nicolai M. Stoye | **Malena dos Santos Guilherme** | **Kristina Endres**

Department of Psychiatry and Psychotherapy, University Medical Center of the Johannes Gutenberg-University, Mainz, Germany

Correspondence
Kristina Endres, Department of Psychiatry and Psychotherapy, University Medical Center of the Johannes Gutenberg-University, Untere Zahlbacher Str. 8, 55131 Mainz, Germany.
Email: Kristina.Endres@unimedizin-mainz.de

Funding information
Stiftung Rheinland-Pfalz für Innovation (Rheinland-Pfalz Foundation for Innovation), Grant/Award Number: 961 - 386261/1129; Alfons Geib-Stiftung

Abstract

Alzheimer's disease (AD) affects around 33 million people worldwide, which makes it the most prominent form of dementia. The main focus of AD research has been on the central nervous system (CNS) for long, but in recent years, the gut gained more attention. The intestinal tract is innervated by the enteric nervous system (ENS), built of numerous different types of neurons showing great similarity to neurons of the CNS. It already has been demonstrated that the amyloid precursor protein, which plays a major role in AD pathology, is also expressed in these cells. We analyzed gut tissue of AD model mice (5xFAD) and the respective wild-type littermates at different pathological stages: pre-pathological, early pathological and late pathological. Our results show significant difference in function of the intestine of 5xFAD mice as compared to wild-type mice. Using a pathway array detecting 84 AD-related gene products, we found ApoA1 expression significantly altered in colon tissue of 5xFAD mice. Furthermore, we unveil ApoA1's beneficial impact on cell viability and calcium homeostasis of cultured enteric neurons of 5xFAD animals. With this study, we demonstrate that the intestine is altered in AD-like pathology and that ApoA1 might be one key player within the gut.

KEYWORDS

A-beta, enteric nervous system, FoxA2, lipids

1 | INTRODUCTION

Over 50 million people currently suffer from dementia worldwide and estimates assume that this number will more than triple over the next 30 years.[1] Already in 2018 the costs for treatment were about one trillion USD.[1] About two thirds of people suffering from dementia are diagnosed with Alzheimer's disease (AD). However, there is still no cure for this fatal disease and only few drugs are available for treatment of AD symptoms.[2] Meanwhile, it is commonly accepted that the accumulation and deposition of amyloid-beta (A-beta) peptides in the brain presents one of the most prominent pathological hallmarks of the disease.[3-5] Changes in A-beta level and distribution are, inter alia, able to induce inflammatory processes, oxidative stress, disbalance in calcium homeostasis and finally can

Abbreviations: A-beta, amyloid-beta; AD, Alzheimer's disease; ApoA1, apolipoprotein A1; CdkII, cyclin-dependent kinase like 1; CNS, central nervous system; ENS, enteric nervous system; GTT, gut transit time; PD, Parkinson's disease; SCFAs, short chain fatty acids; TREM2, triggering receptor expressed on myeloid cells 2.

[Correction added on August 10, 2020, after first online publication: Projekt DEAL funding statement has been added.]

lead to neuronal dysfunction and cell death (reviewed in 4,6). So far, AD is seen mainly as a neurodegenerative disease of the brain, although certain comorbidities such as diabetes[7-10] and loss of weight in late life[11-13] are well known. Recent work shows increasing evidence that besides the brain, also the gut as a peripheral organ might contribute to CNS disorders (reviewed in 14,15). The intestine shows great complexity in its structure which is due to the diverse tasks needed for food digestion and protection against potential pathogens. For managing this variety of functions, the gastrointestinal tract is innervated by its own nervous system, the enteric nervous system (ENS), which is able to act partially autonomous.[16-19] The ENS consists of around 400-600 million neurons in humans, which are organized in mesh-like structures, called plexuses (Auerbach's and Meissner's plexus).[18] It has diverse functions and regulates, for example, motility of the gastrointestinal tract, secretion of gastric acid, blood flow, and nutrition absorbance (for an overview see 16-20). The ENS shows great homology to the CNS not only in its complex structure but also in neurotransmitters used for signal transmission (reviewed in 18). Therefore, it is not surprising that the ENS has already been connected to neurodegenerative diseases. In Parkinson's disease (PD) one of the pathological hallmarks are Lewy bodies, abnormal aggregates of protein with alpha-synuclein as their primary structural component. For PD, it has been shown that one of the drivers of pathology might be the expression of alpha-synuclein in the ENS, from where it migrates to the CNS,[21-23] finally resulting in death of neurons in the brain. Diseases, resulting in the loss of enteric neurons during development such as Hirschsprung's disease are often fatal when not treated (reviewed in 24). In AD, A-beta peptides typically found in the brain of patients, could be demonstrated already decades ago by Joachim and colleagues within selected gut specimen.[25] In experiments with AD model mice, it has been shown that overexpression of A-beta results in an increase of inflammatory markers (eg, COX-2) in the gut of transgenic mice, otherwise typically seen in AD brain samples.[26] Furthermore, a specific loss of nitrergic and cholinergic neurons could be observed in the transgenic mouse model APP/PS1.[27] For a deeper understanding of the gut with its nervous system, and its role in AD, we analyzed four representative gut segments of the 5xFAD mouse model[28] regarding differences in expression of 84 genes involved in AD pathogenesis. The most prominently affected gene product, ApoA1, was further investigated regarding its role in A-beta-driven changes in primary culture of enteric neurons. Furthermore, the modulation of ApoA1 expression by FoxA2, a central regulator of lipid metabolism, was investigated. Finally, we were able to show differences in viability and calcium influx of enteric neurons derived from model mice and the reversal of these impairments by ApoA1 administration.

2 | MATERIALS AND METHODS

2.1 | Animals

For maintenance, male B6SJL-Tg (APPSwFlLon,PSEN1*M146L*L286V)6799Vas/Mmjax (5xFAD) mice (Jackson Lab, Bar Harbor, Maine, USA) were crossbred with female C57BL/6J mice.[28] The animals were group-housed (three to five animals) with a 12 hours day/night cycle. Food and water were available ad libitum. The non-transgenic offspring was used as control. All procedures were performed in accordance with the European Communities Council Directive regarding care and use of animals for experimental procedures and were approved by local authorities (Landesuntersuchungsamt Rheinland-Pfalz; approval number G17-1-035).

2.2 | Tissue sample collection

Male 5xFAD mice and their respective littermates were sacrificed by decapitation after isoflurane anesthesia. The gut was removed and 2 cm long pieces of duodenum, jejunum, caecum, and colon were prepared. These gut pieces were opened longitudinally and carefully rinsed two times with sterile, isotonic NaCl. Samples were collected from three different mice for each gut segment, time point, and genotype regarding the initial expression analysis. For preservation, tissue pieces were submerged in RNA later (Qiagen, Hilden, Germany) and stored at −80°C until RNA preparation was conducted.

For liver tissue, portal vein of sacrificed animals was isolated and flushed with high volumes of ice cold 10 mM Tris/HCl to remove the blood. The median lobe of the liver was utilized for analysis. Crude myenteric plexus preparations (from duodenum to colon) for Western blotting were conducted as described for the first steps of isolation of enteric neurons (see below). Six pieces per mouse were collected from wild-type and transgenic animals and combined per animal before further homogenization.

For serum samples, truncal blood was collected with sacrifice of the animals. After 45 minutes of clotting, serum was obtained by centrifugation and subsequently stored at −80°C until further use.

2.3 | Acetylcholinesterase activity measurement

A colorimetric assay (Ellman's method, 29) was conducted to assess the levels of Acetylcholinesterase. Therefore, small intestine was isolated as described before and whole brain was prepared from approx. 40-week-old male 5xFAD mice and their respective wild-type littermates. Tissue was homogenized with

100 mg/500 μL of potassium phosphate buffer (0.5 M) containing protease inhibitor cocktail (Roche, Basel, Switzerland) with the TissueLyzer LT (Qiagen) for 5 minutes at 50 Hz followed by sonication with 20% output and 10 pulses (UW 2070, Bandelin electronic). After sonication, homogenates were centrifuged at 4°C for 1 minute at 1000 *g*. Supernatant of the small intestine preparations was diluted 1:10 and supernatant of brain tissue preparation 1:100 with potassium phosphate buffer in clear 96-well plates. Acetylthiocholine iodid (Sigma-Aldrich, St. Louis, Missouri, USA) (1 mM) and 5,5′-Dithiobis-2-nitrobenzoic acid (Sigma-Aldrich) (0.25 mM) were added. After 5 minutes incubation time in the dark at RT samples were measured at 405 nm over a period of 125 minutes. Minimum of signal was subtracted from maximum and slope normalized to protein content. Protein content was measured using Roti-Nanoquant (Carl Roth, Karlsruhe, Germany) following the vendor's manual.

2.4 | Gut transition time measurement

For measurement of the gut transition time, wild-type and 5xFAD animals were fed with sky blue solution (PME; 0.58 μL/g body weight). After the feeding, mice were single caged and time till mice defecated blue feces was measured.

2.5 | RNA assay

For qPCR, the RNA concentration of samples obtained from three corresponding animals was adjusted to 75 ng/μL. Three microliters of each RNA-sample was pooled to give a better biological averaging.[30] Eight microliters of this RNA-pool sample was used for reverse transcription using the "RT^2 first strand kit" (Qiagen) following the manufacturer's instructions. The obtained cDNA was subjected to the RT^2 Profiler PCR Array (Qiagen) according to the manufacturer's instruction. Levels of RNA were normalized to at least three different housekeeping genes, selected out of five potentially applicable housekeeping genes on the array by the least variation within the respective tissue. Changes in mRNA level were designated as "hit", if effect size was greater than the mean variation of the corresponding housekeeping genes. The expression of transcription factors and Abca1 was analyzed using the QuantiTect SYBR Green RT-PCR Kit (Qiagen) following the manufacturer's instructions using 100 ng RNA per reaction and the respective QuantiTect Primer Assay (Qiagen).

2.6 | Western blotting

Gut, liver, and plexus preparation were carried out as described before. The rinsed tissue specimen was subjected to Tris-HCl buffer (10 mM, pH 8) with protease inhibitor cocktail (Roche) (200 μL/100 mg of tissue), snap frozen in liquid nitrogen, and stored at −80°C until further usage. Samples were homogenized and protein content was determined as described before. Protein concentration was adjusted to 30 μg per 15 μL in LDS NuPAGE buffer (1x, Life Technologies) containing DTT (1 M, 10% v/v). The solution was boiled for 5 minutes at 95°C. Proteins were separated on a 10%- or 14%- (for A-beta detection) SDS polyacrylamide gel and proteins were transferred to a nitrocellulose membrane (GE Healthcare). The membrane was blocked with I-block solution (0.2% in PBS) (Thermo Fisher Scientific) including 0.05% Tween 20 (AppliChem, Darmstadt, Hessen). Primary antibody incubation took place overnight at 4°C with antibody against ApoA1 (Thermo Fisher Scientific; for a specificity control of the antibody see Figure S1) or against GFAP (Cell Signaling) with a dilution of 1:1000 in blocking solution. Actin or GAPDH detection was used as loading control (antibodies from Sigma-Aldrich and Cell Signaling). For A-beta detection, antibody 6E10 (Covance) was used. The respective secondary antibody, coupled with horseradish peroxidase, was applied (Thermo Fisher Scientific) and light signals were detected after incubation with SuperSignal West Femto chemiluminescent substrate (Thermo Fisher Scientific) using a CCD-camera imaging system (Stella Camera, Raytest, Straubenhardt, Germany).

2.7 | A-beta/ ApoA1 interaction

To investigate the interaction of ApoA1 (in 10 mM NH_4HCO_3; Chemicon International, Temecula, USA) with A-beta (in 5 mM NH_4OH, PBS buffered; AnaSpec, Fremont California, USA) or BSA (in 5 mM NH_4OH, PBS buffered; Carl Roth), proteins were incubated with solvent or in the molar ratio of 1:10 as described before.[31] Formation of complex was detected using 4%-20% Mini-PROTEAN TGX Precast Gels (Bio-Rad, Hercules California, USA) under native conditions. PAA-Gels were silver-stained using the Roti-Black P kit (Carl Roth) following the vendor's recommendation.

2.8 | A-beta aggregation assay

For the A-beta aggregation assay, human AggreSure A-beta (1-42; 23.6 μM; AnaSpec) and Thioflavin T (250 μM; Sigma) were combined in 50 mM Tris/150 mM NaCl (pH 7.2). To investigate the influence of ApoA1 on A-beta aggregation, the mixture was incubated with either ApoA1 (2.4 μM) or morin (0.1 mM in ethanol; Sigma) or the respective solvent control on black 384-well plates (Greiner Bio-One, Kremsmünster, Austria). Fluorescence was measured at 37°C for a period of 40 minutes every minute, with shaking in between with the Fluostar Omega (BMG Labtech, Cary, NC, USA)

(Ex/Em = 440/484 nm). For long-term observation, single measurements were performed at the indicated time points. In between, samples were kept under constant shaking (300 rpm) at 37°C in the dark.

2.9 | Lipid extraction from mouse feces

Mice were moved to a fresh cage. After 24 hours, fecal pellets were collected in the morning. Lipid extraction was done according to Kraus et al, 2015[32] (modified Folch extraction). In brief, 5 mL of saline were added to 1 g of mouse feces and mixed with chloroform in methanol (2:1 by volume). The suspension was centrifuged at 1000 *g* for 10 minutes at 21°C and the lipid phase removed. After the liquid was evaporated, lipid mass was calculated in weight of lipids/ total feces weight.

2.10 | HDL/ LDL-VLDL assay

The kit was used as recommended by the manufacturer for the fluorometric procedure (Sigma-Aldrich). In brief, 10 µL of serum were subjected to precipitation; subsequently 3 µL from 10-fold dilutions were used for measurement of fraction-dependent cholesterol with the Fluostar Omega (BMG Labtech).

2.11 | Isolation of primary enteric neurons

Enteric neuron isolation was carried out with slight changes according to Smith and colleagues.[33] Briefly, 2- to 3-month-old mice were sacrificed as described before. The whole gut was dissected, the small and the large intestine were kept in carbogen-gassed Krebs buffer, and the caecum was discarded. Each segment was rinsed with 10 mL of Krebs buffer from each side and cut into segments of approximately 2 cm length. The longitudinal muscle layer was peeled off with a cotton swab and the tissue was washed by centrifugation in 1 mL of Krebs buffer three times at 350 *g* for 30 s at 4°C. After centrifugation, the tissue was digested in collagenase solution (1.3 mg/mL; Worthington, Lakewood, New York) for 1 hour at 37°C under gentle agitation while being carbogen-gassed. Afterwards, tissue homogenate was centrifuged at 400 *g* for 10 minutes at 4°C, and digested with a sterile 37°C warm, 0.05% trypsin (Gibco)/ PBS solution. Digestion was stopped by adding DMEM/F12 supplemented with 10% FCS, 1% Glutamine and 1x Antibiotic/Antimycotic (all Life Technologies GmbH). Cells were centrifuged at 400 *g* for 10 minutes at RT. After centrifugation, the cell pellet was resuspended in neuronal medium (Neurobasal A with B-27, 2 mM L-glutamine, 1% FCS, 10 ng/mL of GDNF, and 1x Antibiotic/Antimycotic; all Life Technologies) and filtered through a 100 µm cell strainer (Greiner bio-one). The filtered cells were incubated on a rotation mixer for 30 minutes at 4°C. After mixing, cells were washed with 3 mL of neuronal medium and then centrifuged at 400 *g* for 10 minutes at RT. Cells obtained from one gut were resuspended in 600 µL of neuronal medium; for a 24-well plate (Sarstedt AG & Co. KG, Nümbrecht, Germany) 100 µL of neuron-containing suspension were added to 750 µL of neuronal medium in one well, coated with Poly-L-Lysine hydrobromide (PLL, Sigma-Aldrich Chemie GmbH). After 4 days in culture experiments were conducted.

2.12 | Cell culture

Primary enteric neurons were cultivated in neurobasal A DMEM/F12 supplemented with 1% FCS, 1% Glutamine, 1x B-27, 1x Antibiotic/Antimycotic (all: Life Technologies), 10 ng/mL of Glial Derived Neurotrophic Factor (Acris, Herford, Germany) at 5% CO_2, 37°C in humidified air (95%).

2.13 | Toxicity assay

About 112.5 µL of medium were pipetted into PLL coated black glass-bottom 96-well plates and 15 µL of cell suspension (see above) were added. After an incubation period of 48 hours half of the medium was aspirated and 36.25 µL of fresh medium were added, supplemented with either 2.5 µM A-beta$_{42}$ (AnaSpec), or as control 2.5 µM scrambled A-beta$_{42}$ (AnaSpec), or 0.25 µM ApoA1 (Chemicon international) or the respective solvent control (for A-beta or scrambled A-beta 5 mM NH_4OH in 1x PBS, for ApoA1 10 mM NH_4HCO_3).

2.14 | Immunofluorescence

Enteric neurons were seeded on PLL coated coverslips in 24 well-plates. For this purpose, 100 µL of cell suspension (see above) were added to 750 µL of neuronal medium. After 3 days of incubation 50% of cell supernatant was changed. After 4 days of incubation, cells were washed with PBS and incubated for 20 minutes at RT in 4% PFA solution, followed by a second washing step. Cells were stored in 1xPBS at 4°C until being blocked in 1x PBS supplemented with 10% FCS for 1 hour. After blocking, cells were incubated with primary antibody for detection of either β III-tubulin or NeuN (both Cell Signaling Technology) in a 1:500 dilution in blocking solution over night at 4°C. After incubation, cells were washed with PBS and counterstained with DAPI (10 µg/mL; Carl Roth) for 5 minutes at RT followed by three washing

steps with PBS. The incubation with the secondary antibody (Life Technologies) was carried out for 1 hour followed by three PBS washing steps. After this, microscopy of coverslips was carried out using the AxioVert 200M microscope (Carl Zeiss, Oberkochen, Germany).

2.15 | Calcium influx measurement

Calcium influx was measured using the Calbryte 520-AM indicator (AAT Bioquest 20651, Sunnyvale, California, USA) as the vendor recommended. After 4 days of cultivation, 100 µL of 20 mM HEPES buffered HBSS solution containing 10 µM Calbryte 520-AM were added to 100 µL of cell supernatant. Cells were incubated for 45 minutes at 5% CO_2, 37°C, humidified air (95%) followed by a 15 minutes incubation at RT in the dark. After incubation, Calbryte 520-AM containing supernatant was exchanged with HEPES buffered HBSS solution and KCl was added (50 mM) resulting in calcium influx. Binding of calcium to Calbryte 520AM results in a strong fluorescence signal (485 nm excitation, 520 nm emission).

3 | RESULTS

3.1 | Alzheimer's disease-like pathological changes are not restricted to the brain of AD model mice

Changes in gut properties have occasionally been described for AD mouse models such as differences in enteric network density or amount of trypsin in the gut lumen.[34,35] One of the major changes in AD pathology is the activity of the enzyme acetylcholinesterase (AChE) within brain tissue (for a review see 36) which has not been investigated in gut so far to our knowledge. We, therefore, measured the activity of AChE simultaneously in brain and gut tissue of the 5xFAD mouse model for AD using the Ellmans assay.[29] AChE activity was reduced not only in brain homogenates of transgenic animals compared to wild-type littermates, but also in the small intestine of 5xFAD animals (Figure 1A). Cholinergic transmission is an important mediator of gut propulsion in rodents[37,38] and gut transit time is widely used as an indicator for a disturbed intestinal function.[39] Therefore, the gut transit time of 5xFAD and wild-type mice was investigated at three different stages: early pathological (8 weeks), advanced pathological (21 weeks), and late pathological (40 weeks) stage. No difference in gut transit time of 8-week-old mice was observed, but a decreased gut transit time in 21-week-old and 40-week-old 5xFAD animals as compared to their respective wild-type control (Figure 1B). Moreover, GFAP—one of the major indicators of inflammation—likewise showed a significant increase in the gut of aged transgenic animals as compared to same-age littermates (Figure 1C). In sum, this shows the state-dependent influence of the transgenes that have been used for establishing the rodent model, on gut in regard to different functions and physiological pathways. It has already been shown previously, that transgenic human amyloid precursor protein (APP) is expressed in the gut of murine AD models.[34,35] To confirm this for the different pathological stages of 5xFAD mice once more, we here analyzed crude myenteric plexus preparations, collected from small and large intestine, by Western blotting (Figure 1D): in transgenic mice of young as well as old age, a more intense protein band was obtained at 4 kDa which would match the monomeric peptide and some higher protein species only visible in the samples from transgenic animals, presumably representing oligomeric forms. However, also in the wild-type tissue specimen signals were observed that are not expected due to the species-selectivity of the antibody 6E10 (only staining human-derived A-beta containing material). This indicates that in gut tissue cross-reactivity might occur and special caution has to be exercised with interpreting findings. The higher protein intensity found in young transgenic animals as compared to older transgenic animals reflects what was found before in regard to mRNA levels.[35]

To investigate the potential time-dependent manifestation of AD hallmarks in tissue of the intestine, we analyzed the expression of 84 different genes (AD RT^2 Profiler PCR Array, Qiagen), linked to this disease. Investigation took place in four different gut segments at three different time points in the 5xFAD mouse model (Figure 1E). As a pre-pathological stage 1-month-old mice, which seem still not to be impaired by the transgene in the gut,[35] were investigated. Although 2-month-old mice showed no impairment in the gut transit time measurement, general pathological hallmarks such as soluble A-beta in brain are already detectable[28] and therefore, the respective time point was chosen as a stage for an early onset of pathology. At 6 months of age, neuronal loss is starting in the brain of 5xFAD mice[40]; therefore, 8 months were chosen to represent a manifest stage in AD pathology. Most genes within the array were expressed in gut tissue and over all, a minimum of 88% of the AD-linked genes fulfilled quality requirements to be included in further analyzes (Figure S2). Intuitively, a first glance was taken on the main genes associated with A-beta such as murine *App*, *Psen*, *Bace*, and *Mapt*.[41] Respective differences in gene expression could be detected at single time points and within single tissue segments but rather inconsistent and with mostly only minor effect size. Murine *App* itself and *Psen1* and *2* were not changed regarding expression over all time points and gut segments. *Bace1* showed only a minor change in expression in jejunum in 2-month-old 5xFAD animals as compared to controls (fold regulation: 1.58). *Bace2* expression

varied greatly over all gut segments and time points. The expression of *Mapt* was lower in caecum of 2-month-old 5xFAD animals as compared to controls (fold regulation: −1.89).The fold regulation of the main genes associated with A-beta is shown in Table S1.

3.2 | Gene expression in colon tissue is altered in AD model mice

It has already been shown that constipation, impaction of intestine, volvulus, and dilatation of the colon (megacolon) are correlated to AD in humans.[42] It is of note that the most differentially expressed gene over all age-groups was also found in colon samples of 5xFAD animals compared to wild-type mice: apolipoprotein A1 (*ApoA1*; Figure 1E). For this reason, colon was chosen for further analysis. *ApoA1* displayed lower expression in 1- and 2-month-old 5xFAD animals (Figure 2A) but interestingly higher expression in 8-month-old 5xFAD animals as compared to wild-type animals (Figure 2B). Cyclin-dependent kinase like 1 (*CdklI*), the second most strongly affected gene, for example, was higher expressed in 1- and 2-month-old animals as compared to wild-type, but showed no altered expression in 8-month-old animals (Figure 2B). As our first analysis was conducted using pooled RNA samples, not allowing for analysis of variation, we subsequently performed measurements regarding individual animals for the identified hits (*ApoA1*, *CdklI*). RNA analysis on samples obtained from single animals confirmed a higher expression of *CdklI* in 1-month-old 5xFAD animals, but not in 2-month-old animals (Figure 2C). No change in expression was observed in 8-month-old animals. For *ApoA1*, the results obtained from pooled RNA were verified for all time points. *ApoA1* was ~90% lower expressed in 1- and 2-month-old animals and 25 times stronger expressed in 8-month-old animals as compared to wild-type control (Figure 2C).

3.3 | Direct influence of A-beta on the expression of *ApoA1*

Amyloid precursor protein has been found to be present in the intestine of animals with the Thy1-driven transgenes APP and PS1[35] and A-beta could be identified in preparations of enteric plexus (Figure 1D). To investigate if A-beta alone is capable of evoking changes in gene expression of *CdklI* and *ApoA1*, primary cultures of murine enteric neurons from the myenteric plexus of wild-type animals were treated with synthetic A-beta$_{42}$ (for the typical mesh-like structure of these neurons formed in vitro see Figure 3A). The neuronal character of the cultured cells was verified via two neuronal markers, NeuN and β-III tubulin (Tuj1), using immunohistochemistry (Figure 3A) and Western blot (Figure S3). Enteric neurons were treated with either monomeric or oligomeric A-beta$_{42}$ or scrambled peptide as control (for demonstration of the inability of the scrambled, biological inactive peptide to aggregate see Figure S4). Neither monomeric nor oligomeric A-beta preparations influenced the expression of *ApoA1* or *CdklI* after 24 hours of incubation (Figure 3B). Since acute A-beta-treatment had no effect on mRNA levels, *CdklI* and *ApoA1* expression was compared between enteric neurons derived from 5xFAD animals and wild-type animals. Thereby, the analyzed enteric neurons were obtained from a situation with persistent exposure to the transgene. The expression of *CdklI* showed no change between groups. However, ApoA1 level was significantly increased in neurons from 5xFAD mice to ~187% of control (Figure 3C). Both results reflect the observations for gene expression in the 8-month-old animals.

To verify that the changes seen on *ApoA1* mRNA level are also present on protein level, Western blot experiments were conducted. ApoA1 protein level was analyzed in colon-homogenates in all three different age-groups. In 1-month-old 5xFAD mice, ApoA1 was reduced to ~40% of the protein level of wild-type animals. In 2-month-old 5xFAD animals protein level of ApoA1 was reduced to ~75% of wild-type animals while in 8-month-old animals protein level of ApoA1 was increased to ~142% (Figure 3D). This does not directly reflect effect sizes of mRNA levels, but direction of effect was consistent with our observations regarding mRNA. The main sources for ApoA1 production are intestine and liver. To ascertain that the observed elevation is not based on effects in liver and subsequent transport via blood stream, ApoA1 levels in liver of 1-month-old mice were assessed: no significant change could be observed when comparing transgenic and wild-type animals (furthest graph on the right and respective Western blot picture in Figure 3D).

The transcription factors FOXA2 and ARP-1 have been identified as majorly regulating ApoA1 expression.[43,44] We, therefore, assessed expression of both within colonic mRNA samples of 1-month-old and 8-month-old mice. While Arp-1 occurred unaltered when comparing wild-type and 5xFAD mice (Figure S5), FOXA2 was reduced to about 50% of wild-type level in young animals. Old 5xFAD animals revealed elevated mRNA level of about three times higher as their respective wild-type controls (Figure 3E); however, this did not reach statistical significance ($P = .09$). Since both, ApoA1 and FOXA2 are main regulators of lipid homeostasis[45,46] relevance of our findings for systemic lipid excretion was analyzed (Figure 3F). 5xFAD animals showed a decrease in fecal lipids of ~30% (4.35 mg/g feces) in the young cohort, while in the old cohort the lipids were increased by ~30% (5.33 mg/g feces) in comparison to wild-type controls (wild-type young: 6.13 mg/g feces and wild-type old: 4.23 mg/g feces). This was accompanied by an increase of total cholesterol in serum in the

young transgenic mice, while the older animals showed a decrease as compared to wild-type littermates (Figure 3G). An elevated amount of ApoA1 should in consequence also result in elevated amounts of HDL-cholesterol as ApoA1 is the main protein moiety of HDL: although the results did not reach statistical significance, a tendency of increased HDL-cholesterol and a decrease of LDL/VLDL-cholesterol could be observed in the old animals.

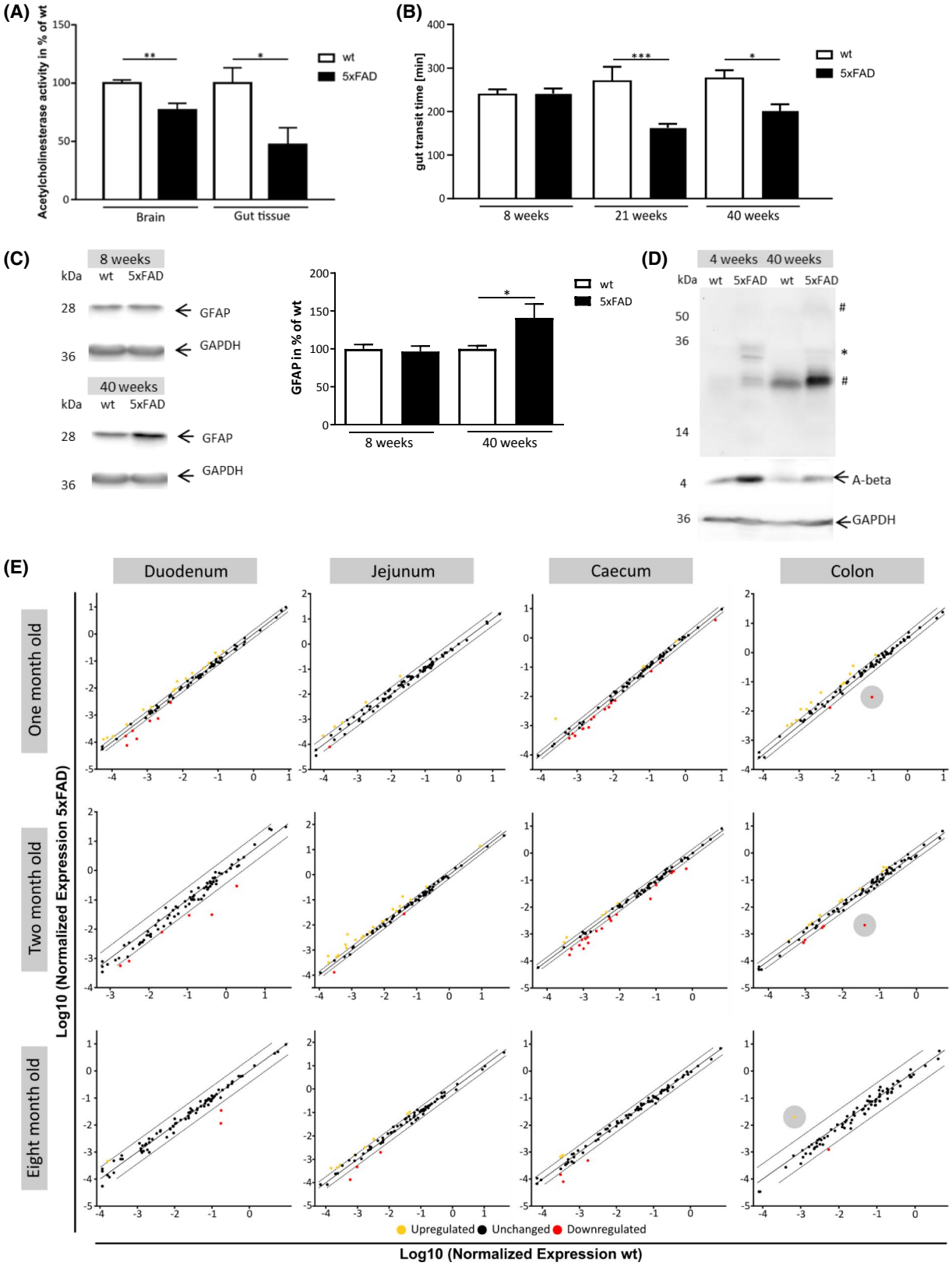

FIGURE 1 Neuronally expressed FAD transgenes (APP/PS1) induce major changes in the gut of Alzheimer's disease model mice. A, Activity of acetylcholinesterase was measured in tissue samples of whole brain and small intestine in 5xFAD and wild-type animals about 40 weeks of age. Values are presented as mean + SEM in % of values obtained from wild-type. Statistical analysis: Unpaired Student's *t* test (***P* < .01; **P* ≤ .05; n ≥ 5). B, Gut transit time (GTT) was monitored using an orally applied stain inert to resorption in animals at three different ages (8, 21, and 40 weeks; males and females evenly matched in every group). Values are presented in minutes (mean + SEM). Statistical analysis: One-Way ANOVA with Bonferroni's multiple comparisons test (***P* < .01; **P* ≤ .05; n ≥ 7). C, Analysis of GFAP expression in colonic tissue was conducted by Western blotting with homogenates from mice aged 8 or 40 weeks. Values have been normalized on GAPDH-dependent signal and are presented as mean + SEM. Statistical analysis: One-Way ANOVA with Tukey's multiple comparisons test (**P* ≤ .05; n = 7 for 8 weeks, n = 5 for 40 weeks). D, Detection of A-beta in crude myenteric plexus preparations was performed by Western blotting. An exemplary picture of A-beta- and GAPDH-signal from the respective samples is shown. In addition to specific signals (A-beta monomers and oligomeric forms, labeled by an asterisk) also unspecific signals were obtained (#), which might be based on the "mouse-on-mouse" incubation with antibody 6E10. E, Investigation of 84 Alzheimer's disease-relevant gene products in four different gut sections at three different ages was carried out with pooled RNA of 5xFAD or wild-type animals (three different male donors each). Dashed lines indicate borders set to identify upregulated (yellow), downregulated (red), and unchanged (black) gene expression. Borders were defined using the variation in expression of at least three housekeeping genes. The grey circle marks the most prominent differently expressed gene product, observed at all three stages of age (*ApoA1*)

In our initial screening (Figure 2), also Abca1 was identified as being differentially regulated in the transgenic animals at early stages in the gut as compared to wild-type controls. Abca1 acts as a receptor for ApoA1 and has also been shown to regulate its lipidation.[47,48] To proof, if the observed effects on lipid excretion solely are based on altered Apoa1 amount or if its receptor might contribute to it, we finally analyzed Abca1 expression in colon tissue as well. With 1 month of age Abca1 expression was not affected by the FAD transgenes; however, with 2 months of age a significant increase was observed (Figure 3H). In the oldest mice investigated, expression levels returned to wild-type levels.

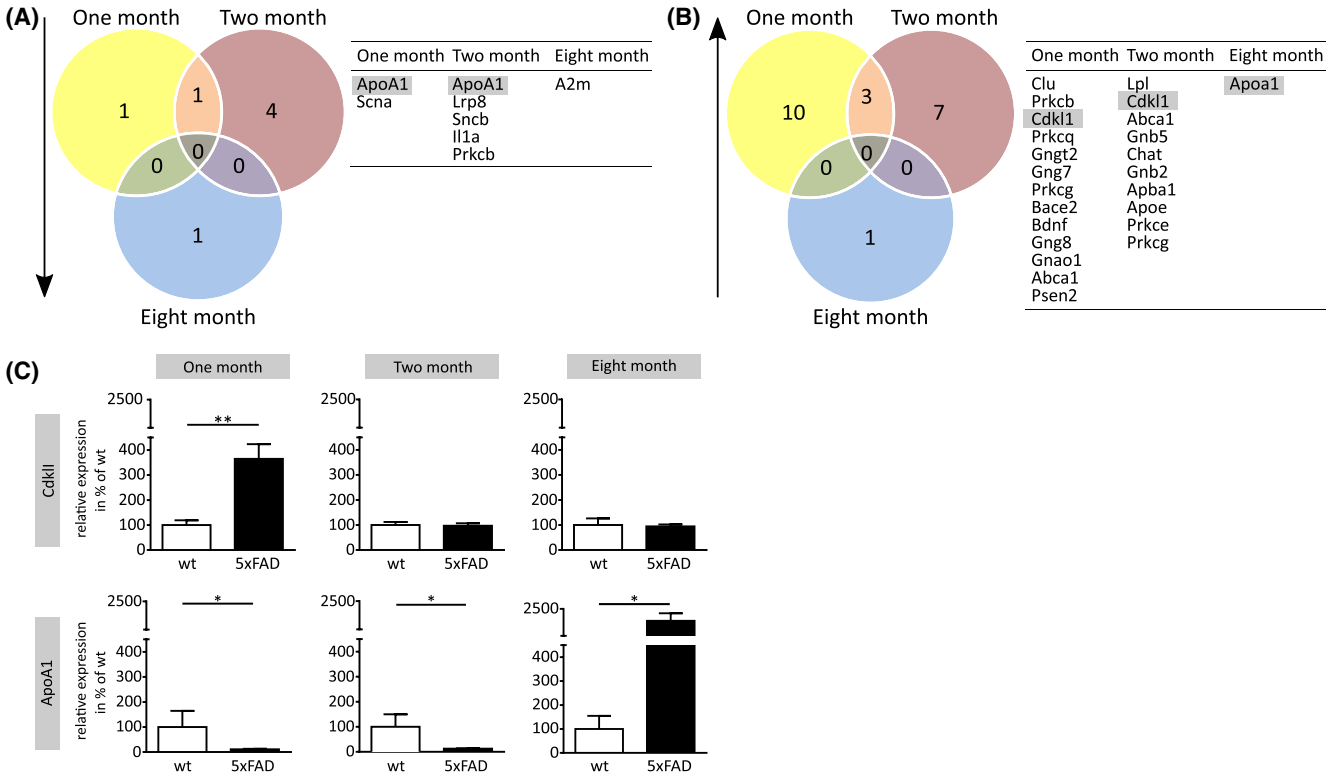

FIGURE 2 Colon shows an altered mRNA expression of AD-relevant genes. A and B, Up- and downregulated genes of animals were analyzed in three different age groups in colonic tissue. Analysis of downregulated genes is shown in A, upregulated genes in B. *ApoA1* showed the strongest downregulation in 1- and 2-month-old animals and the most upregulation in 8-month-old animals. *CdklI* showed the strongest upregulation in 1- and 2-month-old animals; both are marked in grey. C, For improvement of statistical validity of the experiments, mRNA of additional animals was used for single qRT-PCR reactions. Values are normalized to three different housekeeping genes and are shown as mean + SEM in % of values obtained from wild-type animals (statistical analysis: Mann-Whitney test; ***P* ≤ .01; **P* ≤ .05; n ≥ 6 animals for 1 and 2 months; n ≥ 3 animals for 8 months)

3.4 | ApoA1 interacts with A-beta

To further illuminate the role of ApoA1 in AD-like pathology, the potential effect of ApoA1 on typical pathological processes was investigated. A-beta monomers have been shown to be neurotoxic.[49] They are the predominant amyloid species synthesized by neurons[50] and since between monomeric and oligomeric A-beta there was no difference observed in modulating *ApoA1* expression, all further experiments were conducted with monomeric A-beta. To demonstrate that ApoA1

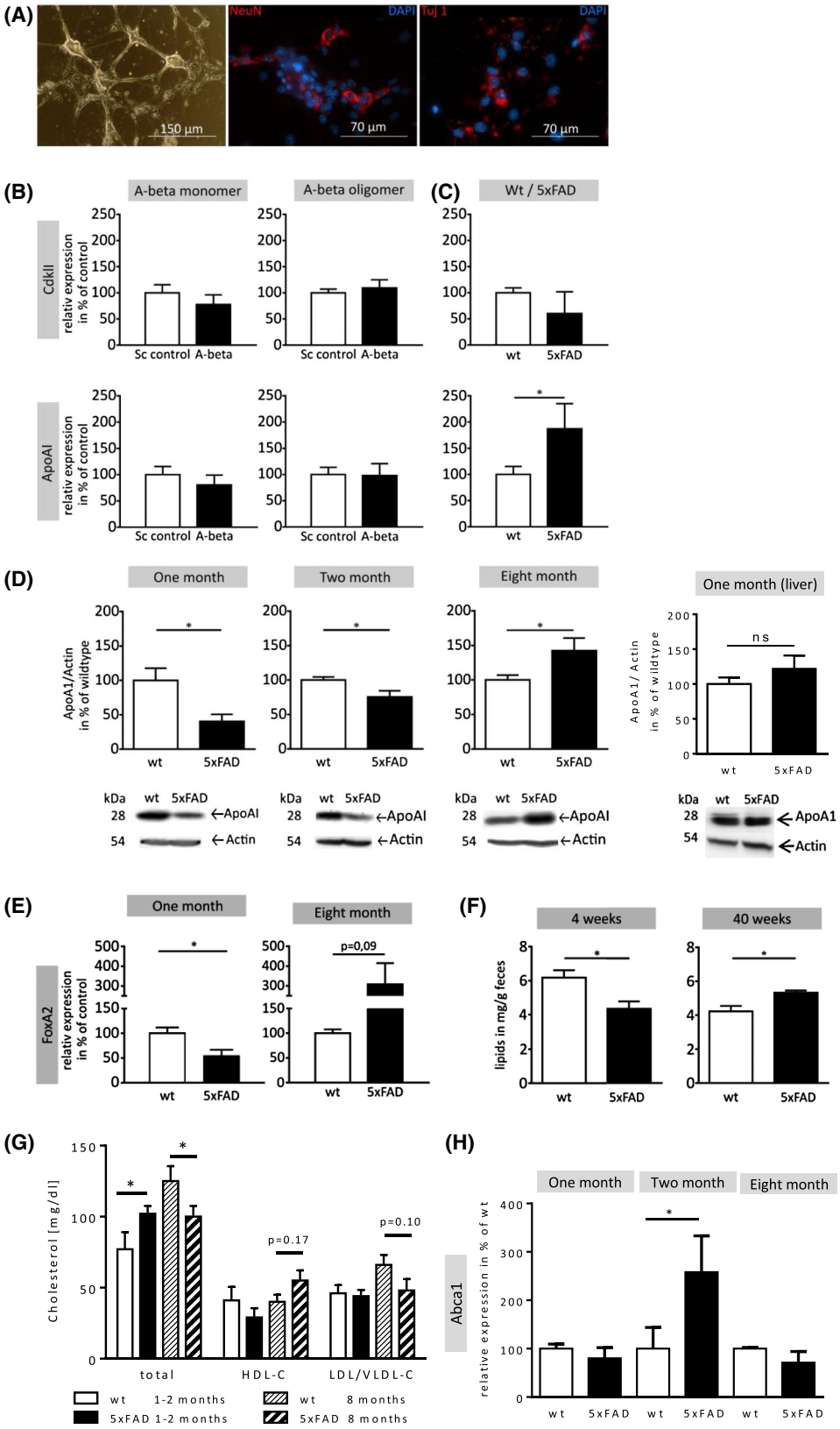

FIGURE 3 ApoA1 expression in enteric neurons is modulated due to chronic overexpression. A, Phase contrast image of cultured enteric neurons grown in typical mesh-like structure. Immunostaining of enteric neurons with neurospecificity markers NeuN and β-III tubulin (Tuj1) in red and DAPI as nuclei counterstain in blue, was carried out. B, Expression of *CdkII* and *ApoA1* was investigated in cultured enteric neurons of wild-type animals. Cells were treated with 2.5 μM monomeric or oligomeric A-beta or scrambled peptide (Sc control) for 24 hours and expression was compared between groups using qRT-PCR. C, In addition, gene expression was assessed by analyzing *CdkII* and *ApoA1* in enteric neurons of 5xFAD as compared to wild-type animals. Values are presented as mean + SD in % of values obtained from control. Statistical analysis: Unpaired Student's *t* test (*$P \leq .05$; $n \geq 4$ different donor animals). D, ApoA1 protein amount was evaluated using densitometric analysis of Western blot images. Values obtained for ApoA1 were normalized to values obtained for Actin. Statistical analysis: Unpaired Student's *t* test (*$P \leq .05$; $n \geq 4$ donor animals per group). E, Gene expression of *FoxA2* was investigated in colonic tissue of 5xFAD and wild-type mice. Values are normalized to the housekeeping gene *Actin* and are shown as mean + SEM in % of values obtained from wild-type animals (statistical analysis: Unpaired Student's *t* test; *$P \leq .05$; n = 4-8 for old and n = 5 for young animals per group). F, Lipid content in feces was measured for 5xFAD mice and their respective littermates and obtained values were normalized to total weight of feces. Statistical analysis: Unpaired Student's *t* test (*$P \leq .05$; $n \geq 7$ for young and n = 4 for old animals per group). G, Total cholesterol, HDL- and LDL/VLDL-cholesterol were determined by a fluorometric assay using serum samples. Statistical analysis was performed by One-Way ANOVA with Fisher LSD post-test (*$P \leq .05$; n = 4-5 per group). H, *Abca1* mRNA level was determined in colon-derived RNA and normalized to *Actin* mRNA levels. Mean + SEM are shown in % of results for wild-type animals (statistical analysis: One-Way ANOVA with Sidak's multiple comparison test; *$P \leq .05$; n = 4-5 per group)

possesses the property to bind A-beta peptides and modulate A-beta aggregation, ApoA1 and A-beta were co-incubated and aggregation products analyzed on a native PAA-gel. At a molar ratio of 1:10, ApoA1 and A-beta formed high molecular weight aggregates, while incubation of A-beta or ApoA1 alone with the respective solvent only resulted in protein bands in the low molecular range (Figure 4A). Incubation with BSA did not result in formation of protein aggregates indicating specificity of the interaction between A-beta and ApoA1. This confirms earlier findings of Paula-Lima, et al.[31] who were able to show a formation of high protein aggregates if ApoA1 and A-beta were incubated at specific molecular ratio. To further investigate the influence of ApoA1 on A-beta aggregation, we conducted fluorescence-based aggregation assays by incubating A-beta and ApoA1 in the presence of Thioflavin T (Figure 4B). Incubation of A-beta with solvent control showed an increase of A-beta aggregation over 40 minutes as expected. Formation of A-beta aggregates could be inhibited by co-incubation with the aggregation inhibitor morin[51] while ApoA1 alone showed no increase of fluorescence signal over time. Incubation of ApoA1 and A-beta (molecular ratio of 1:10) resulted in an accelerated aggregation (Figure 4C) which also persisted up to 4 d after starting the co-incubation (Figure 4D).

3.5 | Enteric neurons derived from 5xFAD mice show changes in calcium homeostasis and cell viability, reversible by ApoA1

To investigate, if the effect of ApoA1 on aggregation influences the neurotoxic effect of A-beta, enteric neurons of wild-type mice were treated with either 2.5 μM A-beta, 0.25 μM ApoA1 or A-beta and ApoA1 together for 24 hours and cell viability was measured (Figure 5A). Treatment of enteric neurons with A-beta alone resulted in a decrease of cell viability of ~13%. Incubation of cells with ApoA1 showed no influence on cell viability, while co-incubation of enteric neurons with ApoA1 and A-beta lead to an elimination of A-beta-induced neurotoxic effects. To evaluate if the beneficial effect of ApoA1 was still existent in enteric neurons exposed chronically to the transgene, enteric neurons prepared from 5xFAD animals were treated with ApoA1. These neurons showed a ~19% higher viability than solvent-treated cells (Figure 5B), demonstrating that ApoA1's beneficial effect on cell viability is not restricted to acute A-beta exposure. Similar experiments conducted in the neuroblastoma cell line SH-SY5Y revealed that viability was comparably restored, when cells were incubated with A-beta in the presence of ApoA1 (A-beta/ApoA1-treated cells: 101% of control, for comparison of A-beta *vs* A-beta/ApoA1-treated cells: $P = .0002$, data not shown).

A-beta and Presenilin are known to modulate calcium-homeostasis and -signaling of neuronal cells.[3,52-54] For that reason, KCl-induced calcium influx was measured in enteric neurons of 5xFAD animals and their respective wild-type littermates (for an exemplary picture see Figure S6). Enteric neurons of transgenic animals showed a much stronger fluorescent signal increase than their wild-type littermates confirming hyper-activity of calcium signaling (Figure 5C). Incubation of these hyperactive enteric neurons with ApoA1 resulted in a ~28% decrease as compared to the solvent treated control (Figure 5D), which indicates that ApoA1 can at least partially restore calcium homeostasis.

4 | DISCUSSION

Although AD is mainly still seen as a neuronal disease of the brain, the gut gains more and more attention in this field of research. In this study we investigated the gut with its enteric nervous system regarding its role in AD. We were able to show a decrease in acetylcholinesterase activity in whole brain homogenates of 5xFAD mice, which is also observed

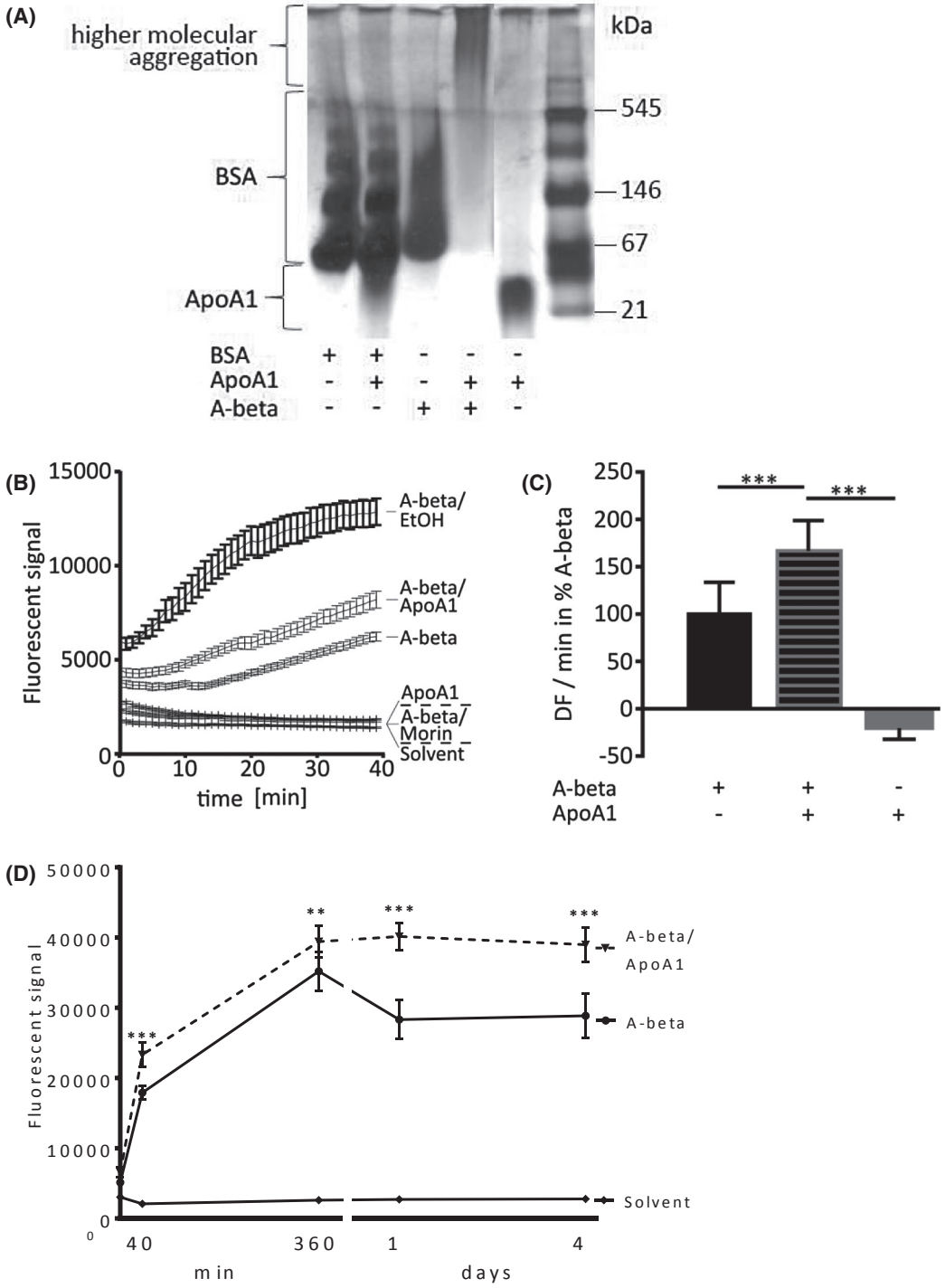

FIGURE 4 Interaction of ApoA1 and A-beta in vitro. A, ApoA1 was incubated with either BSA, human A-beta, or solvent for 24 hours at 37°C and loaded on a native PAA-gel. A couple of protein bands visualized at the same height as the BSA bands occurs in the lane where only A-beta has been subjected to. As these bands also are present in lanes where scrambled A-beta, which is not prone to aggregation, is run (data not shown), we assume that this is not aggregated peptide but material due to the purification process of the vendor (AnaSpec). B, To investigate a potential effect on A-beta aggregation, Thioflavin T was added to the indicated combination. Morin—an aggregation inhibitor—served as control. The respective slope of the fluorescent signal was calculated (C). Values are presented as mean ± SD (values obtained from A-beta without additives set to 100%). The experiment was conducted three times independently. Statistical analysis: One-Way ANOVA with Bonferroni's multiple comparisons test (***$P < .001$; n ≥ 5). D, For long-term effect of ApoA1 in the co-incubation experiment, single measurements were conducted at $t = 0$ and $t = 40$ minutes as well as after 1 and 4 days. In between the measurements, samples were incubated at 37°C under constant shaking. Values are presented as mean ± SD (n = 4). Statistical analysis: Two-Way ANOVA Dunnett's multiple comparisons test (only comparisons between A-beta and A-beta/ApoA1 are shown; ***$P < .001$; **$P < .01$)

in brain homogenates of AD patients.[36,55,56] More interestingly, we could also demonstrate the decrease of AChE in the small intestine of 5xFAD mice, which confirmed the impact of AD on the enteric nervous system since this enzyme is mandatory for the acetylcholine-mediated signal transmission in the ENS.[57-60] This reduction might be of value for AD diagnosis since intestine biopsies are conducted on a regular basis for cancer screening in the elderly and might offer the possibility to study AChE levels of the enteric nervous system in people at risk.[61] To investigate if there is impairment in gut function and if this disease-driven change may already be recognizable at an early stage in disease progression, we analyzed the gut transit time (GTT). This motility test is the most basic tool used to assess disorders of the gut[39,62] and has already been linked to psychiatric disorders such as anxiety and depression.[63] GTT was changed at an age of 21 weeks in 5xFAD animals: at that time point mice display cortex-dependent learning memory stabilization impairments but no restriction in short-term memory (starting at 6 months of age).[64] Forty-week-old mice with severe AD-like pathology also displayed reduced gut transit time, indicating that the gut function is changed during the progression of the disease in 5xFAD animals. The microbiome is responsible for the digestion of dietary fibers to mainly short chain fatty acids (SCFAs).[65] These SCFA have multiple effects and are able to modulate enteric neuron properties (eg, butyrate interacts with the cholinergic system of the gut) which results, for example, in gut motility enhancement.[66,67] It has been shown, that the gut microbiome composition of 5xFAD mice differs from that of wild-type littermates,[35,68] and therefore might play an important role in modifying gut motility. It should be noted that an altered gut transit time is of major importance for further investigations of fecal microbiota in 5xFAD animals, since faster transit time itself has an impact on microbiota composition of the feces.[69]

The effect of an altered gut transit time and the reduced AChE activity in the gut underline the interplay of the intestine and AD-like pathology. In this study we investigated the gut with its ENS regarding expression of 84 AD-related gene products in the 5xFAD mouse model. We found *ApoA1* as the most differentially expressed gene product over all investigated gut segments of this animal model. ApoA1 is a 28 kDa lipoprotein synthesized mainly by the liver and the intestine.[46,70] Literature is not fully consistent regarding the role ApoA1 might have in AD: several reports show a decreased level in serum and plasma of patients with AD,[71,72] or even years before onset of AD.[73] However, there are also reports describing unaltered levels in brain parenchyma or even lowered levels in serum.[74,75] In addition, functional impact is not clear: the level of plasma ApoA1 was, for example, not found to correlate with cognitive function at baseline or with risk of dementia during follow-up in a case-cohort study nested within the Ginkgo Evaluation of Memory Study[76]

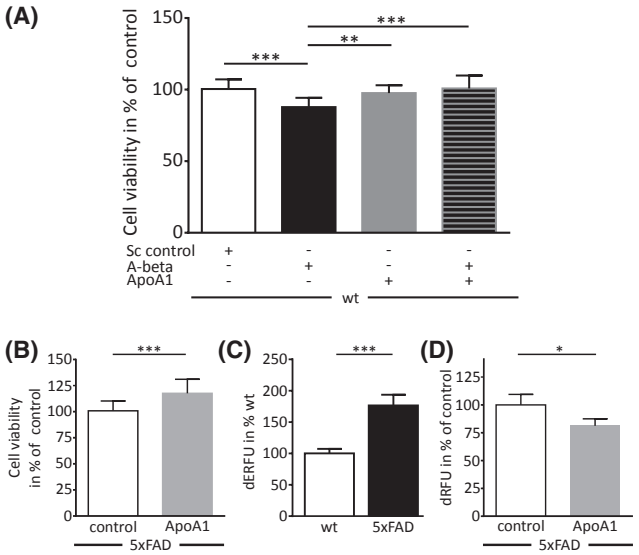

FIGURE 5 ApoA1 has an impact on cell viability of enteric neurons and plays a role in calcium signaling pathways. A, Enteric neurons of wild-type animals were treated with A-beta, ApoA1 or a combination of both. Scrambled A-beta served as a control. After 24 hours of incubation, cell viability was assessed. Values are shown as mean + SD in % values of Sc control. The experiment was conducted with five donor animals. Statistical analysis: One-Way ANOVA with Bonferroni's multiple comparisons test (***$P < .001$; **$P \leq .01$; $n \geq 12$). B, Enteric neurons prepared from 5xFAD mice were incubated with ApoA1 (0.25 μM, 24 hours) as described before and cell viability was assessed. Four independent experiments with four different donor mice were conducted. Statistical analysis: Unpaired Student's *t* test (***$P \leq .001$; $n \geq 19$). C, Calcium influx in wild-type and 5xFAD enteric neurons was measured by a calcium-dependent fluorescence dye and slope of the signal was calculated. Values are expressed as % values obtained for wild-type. The experiment was carried out five times with five donor animals. Statistical analysis: Unpaired Student's *t* test (***$P \leq .001$; $n \geq 21$). D, Enteric neurons of 5xFAD animals were treated with 0.25 μM ApoA1 for 24 hours. Calcium influx was measured and slope calculated. Values are shown as mean + SD in % of values of control obtained in three independent experiments. Statistical analysis: Unpaired Student's *t* test (*$P \leq .05$; $n \geq 16$)

while another earlier study concludes, patients with high concentration of ApoA1 in serum have a lower risk to suffer from AD later in life.[77] In addition, changes in ApoA1 CSF level might even report on general degenerative processes and not specifically on AD-related changes as this protein in CSF was—in our hands—not able to discriminate between a small panel of non-AD and AD-demented individuals.[78]

Here, we were able to demonstrate lower expression of *ApoA1* and reduced protein content in colon tissue of 5xFAD at a pre- and early pathological state while liver was not affected. Investigations in APP/PS1Δ9 mouse model for AD showed that a deficiency in *ApoA1* increases cognitive deficits due to higher A-beta levels in the vascular system,[79] whereas overexpression of *ApoA1* was able to preserve

cognitive function[80] in APP/PS1 mice. Additionally, it has been demonstrated in mouse models of AD that intravenous treatment with ApoA1 reduced cerebral deposition of A-beta.[81] Recently, an investigation of ApoA1 deficiency in APP/PS1 AD model mice revealed increased total and vascular A-beta deposition as well as astrocytosis in comparison to hemizygous controls.[82] This suggests that ApoA1-containing HDL can reduce amyloid-driven pathology and astrocyte reactivity. This effect might be due to ApoA1s ability to bind A-beta and accelerate the formation of higher molecular aggregates which are not neurotoxic.[83,84] While earlier reports described an inhibition of A-beta$_{40}$ aggregation by ApoA1,[85] Paula-Lima and colleagues showed that a different effect occurs in dependency from stoichiometric ratios[31]: at low molar ratio of ApoA1 (20:1 A-beta: ApoA1) ThT-evoked signal was reduced in an *in vitro* aggregation assay. However, at higher ratio (2:1 A-beta: ApoA1 molar ratio) shorter, curvilinear and thinner structures were built and ThT binding was increased. In our experiment, where we used a 10:1 ratio, ApoA1 likewise increased the ThT signal in comparison to samples only containing A-beta and this remained stable for 4 days. Consistent with this finding, ApoA1 used in the same molar ratio was able to neutralize A-beta–induced neurotoxic effects within enteric neuron primary cultures. Moreover, ApoA1 seems to reverse already existing neurotoxic effects induced in enteric neurons of 5xFAD animals.

Interestingly, we found the inverse effect of ApoA1 protein content and gene expression at the late pathological state of 5xFAD animals. The 5xFAD animal model is a rapid model with fast development of pathology. Eight-month-old animals display a severe pathological state with neuronal loss, cognitive impairment, and inflammation which are not observed in 2-month- or 1-month-old animals.[28,86] Therefore, levels of ApoA1 might be increased as part of an inflammatory response since ApoA1 possesses anti-inflammatory properties[87-92] which would also fit our observation of elevated GFAP in the colon of aged transgenic animals. Additionally, this elevation may contribute to neuronal regeneration which is continuously taking place in the enteric nervous system.[93] Like this late phase of AD, the secondary phase of traumatic CNS injury also is characterized by neuronal loss and inflammation and has even been associated with AD.[94-98] Sengupta et al[99] were able to show an increase of ApoA1 in serum of patients in the secondary phase of traumatic spinal cord injury. Moreover, a similar effect has been observed in scratch-wounded neuroblastoma cells: while ApoA1 decreased immediately after the injury, later-on it increased, which was interpreted as a self-protecting mechanism of the injured system.[99] While the neuronal cell line showed this behavior due to acute injury within hours, it is plausible that in the more complex mouse model such regulations occur in a slower time frame over months. An increased ApoA1 expression was also observed in cultured enteric neurons of 5xFAD animals when compared to wild-type animals. The fact that ApoA1 expression is not altered in enteric neurons exposed 24 hours to the recombinant peptide, but in neurons of transgenic animals, indicates that A-beta is not acting on transcription of ApoA1 directly. However, *FoxA2* was shown to mirror the expression level of *ApoA1* in 5xFAD mice: in young mice of 1 month of age it was decreased, while it increased in aged mice. FOXA2 is a major regulator of glucose and lipid metabolism.[100] Interestingly, it also has been described to be elevated in iPSC-based AD cellular models.[44] In midbrain, FOXA2 mediates important function in development and maintenance of murine dopaminergic neurons.[101,102] As dopaminergic neurons have been shown to strongly affect gut transit time,[103] disturbed FOXA2 homeostasis at later age in 5xFAD mice might also be the underlying mechanism for the here observed increased propulsion. For cholinergic transmission a direct link between FOXA2 and neuronal activity in the gut has not been described yet. However, FOXA2 has been identified as a regulator of α5 nicotinic acetylcholine receptor subunit in murine lung organogenesis[104] and this subunit has been shown to stabilize functional nicotinic receptors in at least non-neuronal tissues.[105] While α5 subunit was demonstrated in colonic epithelium of mice and its absence found to increase severity of experimental colitis in knock-out mice,[106] no data regarding enteric neurons are provided so far. Therefore, we cannot undoubtedly conclude that the elevated expression of *FoxA2* directly resulted in the observed faster gut transition via higher activity level of cholinergic neurons.

Nevertheless, faster transit time can directly explain a lower resorption and thereby higher fecal excretion of lipids.[107] This is exactly what we found in aged model mice and which might *vice versa* act on *FoxA2/ApoA1* expression. How the FAD transgenes start this vicious cycle was not resolved so far, however, it is interesting that decreased level of dopaminergic neurotransmitters and dopamine receptors in the CNS have been associated with AD progression.[108] If this is also the case for enteric neurons in AD model mice and patients has to be elucidated in the future. Besides *Apoa1*, also *Abca1* was found to be differentially regulated at 2 months of age in colonic tissue from the 5xFAD mouse model. Its pronounced increase might directly be the consequence of ApoA1 reduction observed at early age as ApoA1 deficiency leads to disturbed cholesterol efflux besides deterioration of other important cellular functions[109]: excess cholesterol accumulation has been shown to induce *Abca1* expression via LXR.[110,111]

How A-beta mediates neurotoxicity is still discussed: it is assumed that amyloid proteins form ion channel pores which disrupt the cellular ion homeostasis.[112-115] Especially calcium permeable channels are formed in membranes resulting in an increase in intracellular calcium concentration.[115-117] This increase in calcium uptake was

also observed in enteric neurons of 5xFAD animals, possibly explaining the neurotoxic effect mediated by A-beta. ApoA1 was significantly reducing calcium uptake of enteric neurons which might explain its neuroprotective effect. Additionally, ApoA1 has been found to be a ligand of the triggering receptor expressed on myeloid cells 2 (TREM2),[118] which loss leads to exacerbated functional decline of neurons in 5xFAD animals.[119]

In summary, we here widen the view on AD as a systemic disease where first molecular changes might not be found in brain but in peripheral tissue such as the gut. While dysfunction of the intestine in PD is a common comorbidity, only within the last years reports on AD mouse models but also patients describe changes in the tissue itself and also in the commensal microbial community. Why these occur is still enigmatic. With our finding that changing ApoA1 levels accompany disease development and thereby evoke changes in enteral lipid excretion, we might contribute to further understanding of this phenomenon. In human brain, evidence for significant ApoA1 mRNA levels is described not to be found and it is assumed that ApoA1 may enter CSF via the choroid plexus.[120-122] Therefore, intestinal ApoA1 production might directly affect the brain. Future investigations have to decipher if our findings from the mouse model also hold true for human patients and if this might open up new avenues for diagnostics.

ACKNOWLEDGMENTS

We thank Beste Senem Degirmenci (Middle East Technical University, Ankara), Julia C. Baumgaertner (Johannes Gutenberg University Mainz), MacKenzie Ellis (Florida State University), and Vu Thu Thuy Nguyen (Johannes Gutenberg University Mainz) for their contribution in the gut transit and lipid experiments; Roland Stauber (Department "Molekulare und Zelluläre Onkologie" of the University Medical Center of the Johannes Gutenberg-University, Mainz) for help and expertise in immunostaining and fluorescence microscopy. This work was supported by the "Stiftung Rheinland-Pfalz für Innovation" and the Alfons Geib-Stiftung. Open access funding enabled and organized by Projekt DEAL.

CONFLICTS OF INTEREST

The authors declare that there is no conflict of interest regarding the contents of this article.

AUTHOR CONTRIBUTIONS

K. Endres initiated the study and conducted the HDL/LDL assay. K. Endres and N.M. Stoye designed the research. N.M. Stoye performed qPCR for AD-related genes, cell culture, and animal experiments. M. dos Santos Guilherme conducted FoxA2 and Arp-1 qPCR, lipid extraction, animal feeding experiments, GFAP and A-beta Western blots and edited the manuscript. K. Endres and N.M. Stoye wrote the manuscript. All authors read and approved the final manuscript.

ORCID

Malena dos Santos Guilherme https://orcid.org/0000-0001-5479-0819
Kristina Endres https://orcid.org/0000-0002-1099-8287

REFERENCES

1. Alzheimer's Disease International. *World Alzheimer Report 2018—The State of the Art of Dementia Research: New Frontiers*. London: Alzheimer's Disease International; 2018.
2. Cummings JL, Morstorf T, Zhong K. Alzheimer's disease drug-development pipeline: few candidates, frequent failures. *Alzheimer's Res Ther*. 2014;6:37.
3. Hardy J, Higgins G. Alzheimer's disease: the amyloid cascade hypothesis. *Science*. 1992;256:184-185.
4. Lane CA, Hardy J, Schott JM. Alzheimer's disease. *Eur J Neurol*. 2018;25:59-70.
5. Hardy J, Selkoe DJ. The amyloid hypothesis of Alzheimer's disease: progress and problems on the road to therapeutics. *Science*. 2002;297:353-356.
6. Haass C, Selkoe DJ. Soluble protein oligomers in neurodegeneration: lessons from the Alzheimer's amyloid β-peptide. *Nat Rev Mol Cell Biol*. 2007;8:101.
7. Arvanitakis Z, Wilson RS, Bienias JL, Evans DA, Bennett DA. Diabetes mellitus and risk of Alzheimer disease and decline in cognitive function. *Arch Neurol*. 2004;61:661-666.
8. Ott A, Stolk RP, van Harskamp F, Pols HA, Hofman A, Breteler MM. Diabetes mellitus and the risk of dementia: the Rotterdam Study. *Neurology*. 1999;53:1937-1942.
9. Peila R, Rodriguez BL, Launer LJ. Type 2 diabetes, APOE gene, and the risk for dementia and related pathologies: the Honolulu-Asia Aging Study. *Diabetes*. 2002;51:1256-1262.
10. Xu W, Qiu C, Gatz M, Pedersen NL, Johansson B, Fratiglioni L. Mid- and late-life diabetes in relation to the risk of dementia: a population-based twin study. *Diabetes*. 2009;58:71-77.
11. Johnson DK, Wilkins CH, Morris JC. Accelerated weight loss may precede diagnosis in Alzheimer disease. *Arch Neurol*. 2006;63:1312-1317.
12. Stewart R, Masaki K, Xue Q-L, et al. A 32-year prospective study of change in body weight and incident dementia: the Honolulu-Asia Aging Study. *Arch Neurol*. 2005;62:55-60.
13. Barrett-Connor E, Edelstein SL, Corey-Bloom J, Wiederholt WC. Weight loss precedes dementia in community-dwelling older adults. *J Am Geriatr Soc*. 1996;44:1147-1152.
14. Mohajeri MH. Brain aging and gut-brain axis. *Nutrients*. 2019;11:424.
15. Mayer EA. Gut feelings: the emerging biology of gut-brain communication. *Nat Rev Neurosci*. 2011;12:453-466.
16. Bayliss WM, Starling EH. The movements and innervation of the small intestine. *J Physiol*. 1899;24:99-143.
17. Gershon MD. The enteric nervous system: a second brain. *Hosp Pract*. 1999;34:31-52.
18. Furness JB. The enteric nervous system and neurogastroenterology. *Nat Rev Gastroenterol Hepatol*. 2012;9:286.
19. Brehmer A. Structure of enteric neurons. *Adv Anat Embryol Cell Biol*. 2006;186:1-91.

20. Furness JB. *The Enteric Nervous System*. Oxford: Blackwell; 2006.
21. Paillusson S, Clairembault T, Biraud M, Neunlist M, Derkinderen P. Activity-dependent secretion of alpha-synuclein by enteric neurons. *J Neurochem*. 2013;125:512-517.
22. Pan-Montojo F, Schwarz M, Winkler C, et al. Environmental toxins trigger PD-like progression via increased alpha-synuclein release from enteric neurons in mice. *Sci Rep*. 2012;2:898.
23. Phillips RJ, Walter GC, Wilder SL, Baronowsky EA, Powley TL. Alpha-synuclein-immunopositive myenteric neurons and vagal preganglionic terminals: autonomic pathway implicated in Parkinson's disease? *Neuroscience*. 2008;153:733-750.
24. Heuckeroth RO. Hirschsprung disease—integrating basic science and clinical medicine to improve outcomes. *Nat Rev Gastroenterol Hepatol*. 2018;15:152-167.
25. Joachim CL, Mori H, Selkoe DJ. Amyloid β-protein deposition in tissues other than brain in Alzheimer's disease. *Nature*. 1989;341:226-230.
26. Puig KL, Lutz BM, Urquhart SA, et al. Overexpression of mutant amyloid-beta protein precursor and presenilin 1 modulates enteric nervous system. *J Alzheimer's Dis*. 2015;44:1263-1278.
27. Han X, Tang S, Dong L, et al. Loss of nitrergic and cholinergic neurons in the enteric nervous system of APP/PS1 transgenic mouse model. *Neurosci Lett*. 2017;642:59-65.
28. Oakley H, Cole SL, Logan S, et al. Intraneuronal beta-amyloid aggregates, neurodegeneration, and neuron loss in transgenic mice with five familial Alzheimer's disease mutations: potential factors in amyloid plaque formation. *J Neurosci*. 2006;26:10129-10140.
29. Ellman GL, Courtney KD, Andres V Jr, Feather-Stone RM. A new and rapid colorimetric determination of acetylcholinesterase activity. *Biochem Pharmacol*. 1961;7:88-95.
30. Kendziorski C, Irizarry RA, Chen KS, Haag JD, Gould MN. On the utility of pooling biological samples in microarray experiments. *Proc Natl Acad Sci U S A*. 2005;102:4252-4257.
31. Paula-Lima AC, Tricerri MA, Brito-Moreira J, et al. Human apolipoprotein A-I binds amyloid-beta and prevents Abeta-induced neurotoxicity. *Int J Biochem Cell Biol*. 2009;41:1361-1370.
32. Kraus D, Yang Q, Kahn BB. Lipid extraction from mouse feces. *Bio Protoc*. 2015;5(1):e1375.
33. Smith TH, Ngwainmbi J, Grider JR, Dewey WL, Akbarali HI. An in-vitro preparation of isolated enteric neurons and glia from the myenteric plexus of the adult mouse. *J Vis Exp*. 2013;78:e50688.
34. Semar S, Klotz M, Letiembre M, et al. Changes of the enteric nervous system in amyloid-beta protein precursor transgenic mice correlate with disease progression. *J Alzheimer's Dis*. 2013;36:7-20.
35. Brandscheid C, Schuck F, Reinhardt S, et al. Altered gut microbiome composition and tryptic activity of the 5xFAD Alzheimer's mouse model. *J Alzheimer's Dis*. 2017;56:775-788.
36. García-Ayllón M-S, Small DH, Avila J, Sáez-Valero J. Revisiting the role of acetylcholinesterase in Alzheimer's disease: cross-talk with P-tau and β-amyloid. *Front Mol Neurosci*. 2011;4:22.
37. Galligan JJ, Burks TF. Cholinergic neurons mediate intestinal propulsion in the rat. *J Pharmacol Exp Ther*. 1986;238:594-598.
38. Delvalle NM, Fried DE, Rivera-Lopez G, Gaudette L, Gulbransen BD. Cholinergic activation of enteric glia is a physiological mechanism that contributes to the regulation of gastrointestinal motility. *Am J Physiol Gastrointest Liver Physiol*. 2018;315:G473-G483.
39. Kim ER, Rhee P-L. How to interpret a functional or motility test—colon transit study. *J Neurogastroenterol Motil*. 2012;18:94-99.
40. Eimer WA, Vassar R. Neuron loss in the 5XFAD mouse model of Alzheimer's disease correlates with intraneuronal Abeta42 accumulation and Caspase-3 activation. *Mol Neurodegener*. 2013;8:2.
41. Giri M, Zhang M, Lü Y. Genes associated with Alzheimer's disease: an overview and current status. *Clin Interv Aging*. 2016;11:665-681.
42. Sonnenberg A, Tsou VT, Muller AD. The "institutional colon": a frequent colonic dysmotility in psychiatric and neurologic disease. *Am J Gastroenterol*. 1994;89:62-66.
43. Ladias JA, Karathanasis SK. Regulation of the apolipoprotein AI gene by ARP-1, a novel member of the steroid receptor superfamily. *Science*. 1991;251:561-565.
44. Wruck W, Schroter F, Adjaye J. Meta-analysis of transcriptome data related to hippocampus biopsies and iPSC-derived neuronal cells from Alzheimer's disease patients reveals an association with FOXA1 and FOXA2 gene regulatory networks. *J Alzheimer's Dis*. 2016;50:1065-1082.
45. Friedman JR, Kaestner KH. The Foxa family of transcription factors in development and metabolism. *Cell Mol Life Sci*. 2006;63:2317-2328.
46. Arciello A, Piccoli R, Monti DM. Apolipoprotein A-I: the dual face of a protein. *FEBS Lett*. 2016;590:4171-4179.
47. Niesor EJ. Will Lipidation of ApoA1 through Interaction with ABCA1 at the intestinal level affect the protective functions of HDL? *Biology (Basel)*. 2015;4:17-38.
48. Nofer JR. Signal transduction by HDL: agonists, receptors, and signaling cascades. *Handb Exp Pharmacol*. 2015;224:229-256.
49. Endres K, Reinhardt S, Geladaris A, et al. Transnasal delivery of human A-beta peptides elicits impaired learning and memory performance in wild type mice. *BMC Neurosci*. 2016;17:44.
50. Larson ME, Lesne SE. Soluble Abeta oligomer production and toxicity. *J Neurochem*. 2012;120(Suppl 1):125-139.
51. Lemkul JA, Bevan DR. Morin inhibits the early stages of amyloid beta-peptide aggregation by altering tertiary and quaternary interactions to produce "off-pathway" structures. *Biochemistry*. 2012;51:5990-6009.
52. Leissring MA, Murphy MP, Mead TR, et al. A physiologic signaling role for the γ-secretase-derived intracellular fragment of APP. *Proc Natl Acad Sci U S A*. 2002;99:4697-4702.
53. Rhee SK, Quist AP, Lal R. Amyloid beta protein-(1–42) forms calcium-permeable, Zn2+-sensitive channel. *J Biol Chem*. 1998;273:13379-13382.
54. Mattson M, Cheng B, Davis D, Bryant K, Lieberburg I, Rydel R. beta-Amyloid peptides destabilize calcium homeostasis and render human cortical neurons vulnerable to excitotoxicity. *J Neurosci*. 1992;12:376-389.
55. Davies P. Neurotransmitter-related enzymes in senile dementia of the Alzheimer type. *Brain Res*. 1979;171:319-327.
56. Perry EK, Tomlinson BE, Blessed G, Bergmann K, Gibson PH, Perry RH. Correlation of cholinergic abnormalities with senile plaques and mental test scores in senile dementia. *Br Med J*. 1978;2:1457-1459.
57. Brookes SJH, Steele PA, Costa M. Calretinin immunoreactivity in cholinergic motor neurones, interneurones and vasomotor neurones in the guinea-pig small intestine. *Cell Tissue Res*. 1991;263:471-481.
58. Holzer P, Holzer-Petsche U. Tachykinins in the gut. Part I. Expression, release and motor function. *Pharmacol Ther*. 1997;73:173-217.

59. Brookes SJH, Steele PA, Costa M. Identification and immunohistochemistry of cholinergic and non-cholinergic circular muscle motor neurons in the guinea-pig small intestine. *Neuroscience*. 1991;42:863-878.
60. McConalogue K, Furness JB. Gastrointestinal neurotransmitters. *Baillieres Clin Endocrinol Metab*. 1994;8:51-76.
61. Lebouvier T, Coron E, Chaumette T, et al. Routine colonic biopsies as a new tool to study the enteric nervous system in living patients. *Neurogastroenterol Motil*. 2010;22:e11-e14.
62. Lin HC, Prather C, Fisher RS, et al. Measurement of gastrointestinal transit. *Dig Dis Sci*. 2005;50:989-1004.
63. Gorard DA, Gomborone JE, Libby GW, Farthing MJ. Intestinal transit in anxiety and depression. *Gut*. 1996;39:551-555.
64. Kimura R, Ohno M. Impairments in remote memory stabilization precede hippocampal synaptic and cognitive failures in 5XFAD Alzheimer mouse model. *Neurobiol Dis*. 2009;33:229-235.
65. den Besten G, van Eunen K, Groen AK, Venema K, Reijngoud D-J, Bakker BM. The role of short-chain fatty acids in the interplay between diet, gut microbiota, and host energy metabolism. *J Lipid Res*. 2013;54:2325-2340.
66. Sochocka M, Donskow-Lysoniewska K, Diniz BS, Kurpas D, Brzozowska E, Leszek J. The gut microbiome alterations and inflammation-driven pathogenesis of Alzheimer's disease—a critical review. *Mol Neurobiol*. 2019;56:1841-1851.
67. Du X, Wang X, Geng M. Alzheimer's disease hypothesis and related therapies. *Transl Neurodegener*. 2018;7:2.
68. Dos Santos Guilherme M, Todorov H, Osterhof C, et al. Impact of Acute and Chronic Amyloid-β Peptide Exposure on Gut Microbial Commensals in the Mouse. *Front. Microbiol*. 2020;. https://doi.org/10.3389/fmicb.2020.01008
69. Tottey W, Feria-Gervasio D, Gaci N, et al. Colonic transit time is a driven force of the gut microbiota composition and metabolism: in vitro evidence. *J Neurogastroenterol Motil*. 2017;23:124-134.
70. Glickman RM, Green PH. The intestine as a source of apolipoprotein A1. *Proc Natl Acad Sci U S A*. 1977;74:2569-2573.
71. Kawano M, Kawakami M, Otsuka M, Yashima H, Yaginuma T, Ueki A. Marked decrease of plasma apolipoprotein AI and AII in Japanese patients with late-onset non-familial Alzheimer's disease. *Clin Chim Acta*. 1995;239:209-211.
72. Merched A, Xia Y, Visvikis S, Serot JM, Siest G. Decreased high-density lipoprotein cholesterol and serum apolipoprotein AI concentrations are highly correlated with the severity of Alzheimer's disease. *Neurobiol Aging*. 2000;21:27-30.
73. Song F, Poljak A, Crawford J, et al. Plasma apolipoprotein levels are associated with cognitive status and decline in a community cohort of older individuals. *PLoS One*. 2012;7:e34078.
74. Harr SD, Uint L, Hollister R, Hyman BT, Mendez AJ. Brain expression of apolipoproteins E, J, and A-I in Alzheimer's disease. *J Neurochem*. 1996;66:2429-2435.
75. Liu HC, Hu CJ, Chang JG, et al. Proteomic identification of lower apolipoprotein A-I in Alzheimer's disease. *Dement Geriatr Cogn Disord*. 2006;21:155-161.
76. Koch M, DeKosky ST, Goodman M, et al. High density lipoprotein and its apolipoprotein-defined subspecies and risk of dementia. *J Lipid Res*. 2020;61:445-454.
77. Saczynski JS, White L, Peila RL, Rodriguez BL, Launer LJ. The relation between apolipoprotein A-I and dementia: the Honolulu-Asia aging study. *Am J Epidemiol*. 2007;165:985-992.
78. Stoye NM, Jung P, Guilherme MDS, Lotz J, Fellgiebel A, Endres K. Apolipoprotein A1 in cerebrospinal fluid is insufficient to distinguish Alzheimer's disease from other dementias in a naturalistic, clinical setting. *J Alzheimer's Dis Rep*. 2020;4:15-19.
79. Lefterov I, Fitz NF, Cronican AA, et al. Apolipoprotein A-I deficiency increases cerebral amyloid angiopathy and cognitive deficits in APP/PS1DeltaE9 mice. *J Biol Chem*. 2010;285:36945-36957.
80. Lewis TL, Cao D, Lu H, et al. Overexpression of human apolipoprotein A-I preserves cognitive function and attenuates neuroinflammation and cerebral amyloid angiopathy in a mouse model of Alzheimer disease. *J Biol Chem*. 2010;285:36958-36968.
81. Fernandez-de Retana S, Montanola A, Marazuela P, et al. Intravenous treatment with human recombinant ApoA-I Milano reduces beta amyloid cerebral deposition in the APP23-transgenic mouse model of Alzheimer's disease. *Neurobiol Aging*. 2017;60:116-128.
82. Button EB, Gilmour M, Cheema HK, et al. Vasoprotective functions of high-density lipoproteins relevant to Alzheimer's disease are partially conserved in apolipoprotein B-depleted plasma. *Int J Mol Sci*. 2019;20:462.
83. Stroud JC, Liu C, Teng PK, Eisenberg D. Toxic fibrillar oligomers of amyloid-β have cross-β structure. *Proc Natl Acad Sci U S A*. 2012;109:7717-7722.
84. Kirkitadze MD, Bitan G, Teplow DB. Paradigm shifts in Alzheimer's disease and other neurodegenerative disorders: the emerging role of oligomeric assemblies. *J Neurosci Res*. 2002;69:567-577.
85. Koldamova RP, Lefterov IM, Lefterova MI, Lazo JS. Apolipoprotein A-I directly interacts with amyloid precursor protein and inhibits A beta aggregation and toxicity. *Biochemistry*. 2001;40:3553-3560.
86. Landel V, Baranger K, Virard I, et al. Temporal gene profiling of the 5XFAD transgenic mouse model highlights the importance of microglial activation in Alzheimer's disease. *Mol Neurodegener*. 2014;9:33.
87. de Seny D, Cobraiville G, Charlier E, et al. Apolipoprotein-A1 as a damage-associated molecular patterns protein in osteoarthritis: ex vivo and in vitro pro-inflammatory properties. *PLoS One*. 2015;10:e0122904.
88. Vuilleumier N, Dayer JM, von Eckardstein A, Roux-Lombard P. Pro- or anti-inflammatory role of apolipoprotein A-1 in high-density lipoproteins? *Swiss Med Wkly*. 2013;143:w13781.
89. Sirnio P, Vayrynen JP, Klintrup K, et al. Decreased serum apolipoprotein A1 levels are associated with poor survival and systemic inflammatory response in colorectal cancer. *Sci Rep*. 2017;7:5374.
90. Cimmino G, Ibanez B, Vilahur G, et al. Up-regulation of reverse cholesterol transport key players and rescue from global inflammation by ApoA-I(Milano). *J Cell Mol Med*. 2009;13:3226-3235.
91. Umemoto T, Han CY, Mitra P, et al. Apolipoprotein AI and high-density lipoprotein have anti-inflammatory effects on adipocytes via cholesterol transporters: ATP-binding cassette A-1, ATP-binding cassette G-1, and scavenger receptor B-1. *Circ Res*. 2013;112:1345-1354.
92. Liao KP, Playford MP, Frits M, et al. The association between reduction in inflammation and changes in lipoprotein levels and HDL cholesterol efflux capacity in rheumatoid arthritis. *J Am Heart Assoc*. 2015;4:e001588.
93. Kulkarni S, Micci MA, Leser J, et al. Adult enteric nervous system in health is maintained by a dynamic balance between neuronal apoptosis and neurogenesis. *Proc Natl Acad Sci USA*. 2017;114:E3709-E3718.

94. Yeh TS, Ho YC, Hsu CL, Pan SL. Spinal cord injury and Alzheimer's disease risk: a population-based, retrospective cohort study. *Spinal Cord*. 2018;56:151-157.
95. Collins JM, King AE, Woodhouse A, Kirkcaldie MT, Vickers JC. The effect of focal brain injury on beta-amyloid plaque deposition, inflammation and synapses in the APP/PS1 mouse model of Alzheimer's disease. *Exp Neurol*. 2015;267:219-229.
96. Anwar MA, Al Shehabi TS, Eid AH. Inflammogenesis of secondary spinal cord injury. *Front Cell Neurosci*. 2016;10:98.
97. Kokiko-Cochran ON, Godbout JP. The inflammatory continuum of traumatic brain injury and Alzheimer's disease. *Front Immunol*. 2018;9:672.
98. Huang SW, Wang WT, Chou LC, Liou TH, Lin HW. Risk of dementia in patients with spinal cord injury: a nationwide population-based cohort study. *J Neurotrauma*. 2017;34:615-622.
99. Sengupta MB, Saha S, Mohanty PK, Mukhopadhyay KK, Mukhopadhyay D. Increased expression of ApoA1 after neuronal injury may be beneficial for healing. *Mol Cell Biochem*. 2017;424:45-55.
100. Wolfrum C, Asilmaz E, Luca E, Friedman JM, Stoffel M. Foxa2 regulates lipid metabolism and ketogenesis in the liver during fasting and in diabetes. *Nature*. 2004;432:1027-1032.
101. Stott SRW, Metzakopian E, Lin W, Kaestner KH, Hen R, Ang S-L. Foxa1 and Foxa2 are required for the maintenance of dopaminergic properties in ventral midbrain neurons at late embryonic stages. *J Neurosci*. 2013;33:8022-8034.
102. Ferri AL, Lin W, Mavromatakis YE, et al. Foxa1 and Foxa2 regulate multiple phases of midbrain dopaminergic neuron development in a dosage-dependent manner. *Development*. 2007;134:2761-2769.
103. Li ZS, Schmauss C, Cuenca A, Ratcliffe E, Gershon MD. Physiological modulation of intestinal motility by enteric dopaminergic neurons and the D2 receptor: analysis of dopamine receptor expression, location, development, and function in wild-type and knock-out mice. *J Neurosci*. 2006;26:2798-2807.
104. Porter JL, Bukey BR, Geyer AJ, Willnauer CP, Reynolds PR. Immunohistochemical detection and regulation of alpha5 nicotinic acetylcholine receptor (nAChR) subunits by FoxA2 during mouse lung organogenesis. *Respir Res*. 2011;12:82.
105. Wessler I, Kirkpatrick CJ. Acetylcholine beyond neurons: the non-neuronal cholinergic system in humans. *Br J Pharmacol*. 2008;154:1558-1571.
106. Orr-Urtreger A, Kedmi M, Rosner S, Karmeli F, Rachmilewitz D. Increased severity of experimental colitis in alpha 5 nicotinic acetylcholine receptor subunit-deficient mice. *NeuroReport*. 2005;16:1123-1127.
107. Fine KD, Fordtran JS. The effect of diarrhea on fecal fat excretion. *Gastroenterology*. 1992;102:1936-1939.
108. Pan X, Kaminga AC, Wen SW, Wu X, Acheampong K, Liu A. Dopamine and dopamine receptors in Alzheimer's disease: a systematic review and network meta-analysis. *Front Aging Neurosci*. 2019;11:175.
109. Kajani S, Curley S, McGillicuddy FC. Unravelling HDL-looking beyond the cholesterol surface to the quality within. *Int J Mol Sci*. 2018;19(7):1971.
110. Wang N, Silver DL, Costet P, Tall AR. Specific binding of ApoA-I, enhanced cholesterol efflux, and altered plasma membrane morphology in cells expressing ABC1. *J Biol Chem*. 2000;275:33053-33058.
111. Venkateswaran A, Laffitte BA, Joseph SB, et al. Control of cellular cholesterol efflux by the nuclear oxysterol receptor LXR alpha. *Proc Natl Acad Sci U S A*. 2000;97:12097-12102.
112. Sakono M, Zako T. Amyloid oligomers: formation and toxicity of Abeta oligomers. *FEBS J*. 2010;277:1348-1358.
113. Sengupta U, Nilson AN, Kayed R. The role of amyloid-β oligomers in toxicity, propagation, and immunotherapy. *EBioMedicine*. 2016;6:42-49.
114. Arispe N. Architecture of the Alzheimer's AβP ion channel pore. *J Membr Biol*. 2004;197:33-48.
115. Arispe N, Diaz JC, Simakova O. Aβ ion channels. Prospects for treating Alzheimer's disease with Aβ channel blockers. *Biochim Biophys Acta*. 2007;1768:1952-1965.
116. Demuro A, Mina E, Kayed R, Milton SC, Parker I, Glabe CG. Calcium dysregulation and membrane disruption as a ubiquitous neurotoxic mechanism of soluble amyloid oligomers. *J Biol Chem*. 2005;280:17294-17300.
117. Murphy M. The molecular pathogenesis of Alzheimer's disease: clinical prospects. *Lancet*. 1992;340:1512-1515.
118. Yeh FL, Wang Y, Tom I, Gonzalez LC, Sheng M. TREM2 binds to apolipoproteins, including APOE and CLU/APOJ, and thereby facilitates uptake of amyloid-beta by microglia. *Neuron*. 2016;91:328-340.
119. Wang Y, Cella M, Mallinson K, et al. TREM2 lipid sensing sustains the microglial response in an Alzheimer's disease model. *Cell*. 2015;160:1061-1071.
120. Elliott DA, Weickert CS, Garner B. Apolipoproteins in the brain: implications for neurological and psychiatric disorders. *Clin Lipidol*. 2010;51:555-573.
121. Stukas S, Robert J, Lee M, et al. Intravenously injected human apolipoprotein A-I rapidly enters the central nervous system via the choroid plexus. *J Am Heart Assoc*. 2014;3:e001156.
122. Halley P, Kadakkuzha BM, Faghihi MA, et al. Regulation of the apolipoprotein gene cluster by a long noncoding RNA. *Cell Rep*. 2014;6:222-230.

SUPPORTING INFORMATION

Additional Supporting Information may be found online in the Supporting Information section.

How to cite this article: Stoye NM, dos Santos Guilherme M, Endres K. Alzheimer's disease in the gut—Major changes in the gut of 5xFAD model mice with ApoA1 as potential key player. *The FASEB Journal*. 2020;34:11883–11899. https://doi.org/10.1096/fj.201903128RR